J|A|C|S COMMUNICATIONS

Published on Web 11/19/2010

Combination of Indene-C_{60} Bis-Adduct and Cross-Linked Fullerene Interlayer Leading to Highly Efficient Inverted Polymer Solar Cells

Yen-Ju Cheng,*,† Chao-Hsiang Hsieh,† Youjun He,‡ Chain-Shu Hsu,*,† and Yongfang Li*,‡

Department of Applied Chemistry, National Chiao Tung University, 1001 Ta Hseuh Road, Hsin-Chu, 30010 Taiwan, and Beijing National Laboratory for Molecular Sciences, CAS Key laboratory of Organic Solids, Institute of Chemistry, Chinese Academy of Sciences, Beijing 100190, China

Received September 13, 2010; E-mail: yjcheng@mail.nctu.edu.tw; cshsu@mail.nctu.edu.tw; liyf@iccas.ac.cn

Abstract: A poly(3-hexylthiophene) (P3HT)-based inverted solar cell using indene-C_{60} bis-adduct (ICBA) as the acceptor achieved a high open-circuit voltage of 0.82 V due to ICBA's higher-lying lowest unoccupied molecular orbital level, leading to an exceptional power-conversion efficiency (PCE) of 4.8%. By incorporating a cross-linked fullerene interlayer, C-PCBSD, to further modulate the interface characteristics, the ICBA:P3HT-based inverted device exhibited an improved short-circuit current and fill factor, yielding a record high PCE of 6.2%.

Polymeric solar cells (PSCs) offer great potential for fabrication of large-area, lightweight, and flexible organic solar cells by using low-cost printing and coating technologies.[1] A conventional bulk heterojunction (BHJ) PSC with an active layer sandwiched by a low-work-function aluminum cathode and a hole-conducting poly(3,4-ethylenedioxylenethiophene):poly(styrenesulfonic acid) (PEDOT:PSS) layer on top of an indium tin oxide (ITO) substrate is the most widely used and researched device configuration. Utilizing this device architecture, devices incorporating a blend of a regioregular poly(3-hexylthiophene) (P3HT) and a fullerene derivative, [6,6]-phenyl-C_{61}-butyric acid methyl ester (PCBM), have achieved power-conversion efficiencies (PCEs) approaching 5%.[2] During the past 2 years, several important low-band-gap polymers with enhanced absorption abilities have appeared. Researchers made a breakthrough in fabricating PSC devices with PCEs of up to 5−7% based on these polymers.[3] Alongside high performance, long-term stability is a primary area of concern for PSCs. Rapid oxidation of the low-work-function metal cathode and etching of ITO by the acidic PEDOT:PSS layer are the most common reasons for instability in conventional unencapsulated devices. An effective approach to ameliorate these problems, and improve device lifetime, is to fabricate inverted PSCs. By reversing the polarity of charge collection in a regular cell, air-stable Ag combined with an adjacent PEDOT:PSS layer can substitute for air-sensitive Al as the anodic electrode for efficient hole collection. Despite a dramatic improvement in operational lifetime, standard inverted PSCs suffer from a trade-off between performance and stability. The relatively lower performance is attributed to the unfavorable energetics and incompatible chemical interfaces. Extensive efforts to improve the efficiency of inverted PSCs by modifying the interface include inserting Cs_2CO_3 to reduce the ITO work function,[4] using metal oxides such as TiO_x and ZnO to function as electron-selecting layers,[5] modifying the TiO_x or ZnO surface with a self-assembled C_{60} monolayer,[6] using MoO_3 as the hole-extracting buffer,[7] and employing an optical spacer to redistribute the optical field intensity.[8] However, PCEs of P3HT/PCBM-based inverted PSCs are mostly in the range of ca. 2− 4%, which is inferior to that of conventional PSCs. So far, PCE values greater than 5% are unreported in any form of inverted PSC. Recently, a cross-linkable polythiophene has been successfully used to improve the thermal stability of a PCS by chemically fixing the optimized morphology of the active layer. Moreover, this cross-linking approach also allows for fabricating a bilayer solar cell device by solution processing.[9] Later on, we reported a cross-linkable fullerene material, [6,6]-phenyl-C_{61}-butyric styryl dendron ester (PCBSD).[10] The formation of a cross-linked PCBSD (C-PCBSD, Figure 1) interlayer allows deposition of a sequential active layer on top of this interlayer without causing interfacial erosion and realizes a multilayer inverted device by all-solution processing. An inverted solar cell device based on an ITO/ZnO/C-PCBSD/PCBM:P3HT/PEDOT:PSS/Ag configuration achieved an enhanced PCE of 4.4% in comparison to the reference device (PCE = 3.5%) without this interlayer.

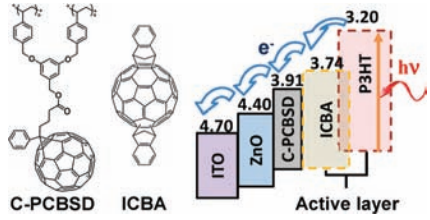

Figure 1. Molecular structure of C-PCBSD and ICBA, and the multilayer structure with LUMO energy levels (in eV) in device **B** (ITO/ZnO/C-PCBSD/ICBA:P3HT/PEDOT:PSS/Ag) for favorable electron collection.

Based on this strategy, further improvement in inverted PSCs performance will rely critically on new development of photoactive materials. One of the major drawbacks of the PCBM/P3HT system is that the energy offset between the highest occupied molecular orbital (HOMO) of P3HT (−5.0 eV) and the lowest unoccupied molecular orbital (LUMO) of PCBM (−3.91 eV) is relatively small. This limits the magnitude of open-circuit voltage (V_{oc}) to around 0.6 V. Considering that commercially available P3HT is the most reliable p-type conjugated polymer that consistently delivers reproducible device characteristics using standard processing conditions, development of a new fullerene derivative possessing a higher-lying LUMO energy level should be a more promising and straightforward way to improve V_{oc} while maintaining other device parameters. Recently, Li and co-workers reported a new n-type fullerene derivative, indene-C_{60} bis-adduct (ICBA, Figure 1).[11] Through double cycloaddition of indene to the core fullerene structure, the LUMO energy level of ICBA can be effectively increased to −3.74 eV, which is 0.17 eV higher than that of single-functionalized PCBM. Because of the enlarged HOMO−LUMO energy offset, the P3HT-based device, incorporating ICBA as the acceptor, achieved a much-enhanced V_{oc} of 0.84 V, yielding an impressive PCE of 6.5%.[11] It is thus highly promising and desirable to explore the potential for utilization of ICBA in high-performance inverted PSC devices. By using ICBA to substitute PCBM

† National Chiao Tung University.
‡ Chinese Academy of Sciences.

10.1021/ja108259n

and act as the acceptor in the active layer, we fabricated a standard inverted device **A** with the configuration of ITO/ZnO/ICBA:P3HT(1:1, w/w)/PEDOT:PSS/Ag. Details of device fabrication and measurement are available in the Supporting Information. Figure 2 shows the $J-V$ characteristics and corresponding external quantum efficiencies (EQEs) of these devices. Encouragingly, the intrinsic higher-lying LUMO energy level of ICBA can be fully translated into the large V_{oc} value of the inverted device. Device **A** achieved $V_{oc} = 0.82$ V, a short-circuit current (J_{sc}) of 10.6 mA/cm^2, and a fill factor (FF) of 55%, yielding a high PCE of 4.81%. This PCE represents a 31% improvement over the corresponding PCBM-based device, with the 3.5% PCE.[10] Following these encouraging results, we fabricated device **B**, (ITO/ZnO/C-PCBSD/ICBA:P3HT(1:1,w/w)/PEDOT:PSS/Ag), incorporating a C-PCBSD interlayer. Under AM 1.5G illumination at 100 mW/cm^2, device **B** exhibited an enhanced $V_{oc} = 0.84$ V, $J_{sc} = 12.4$ mA/cm^2, and FF = 60%, achieving an exceptional PCE of 6.22% which is a 29% increase over device **A** (Figure 2a). Device **B** also had a large EQE maximum of 74%, which is concordant with its high photocurrent (Figure 2b). More importantly, the high performance of device **B** is reproducible. Under the same fabrication conditions, 10 **B**-type devices produced an average PCE of 5.9%.

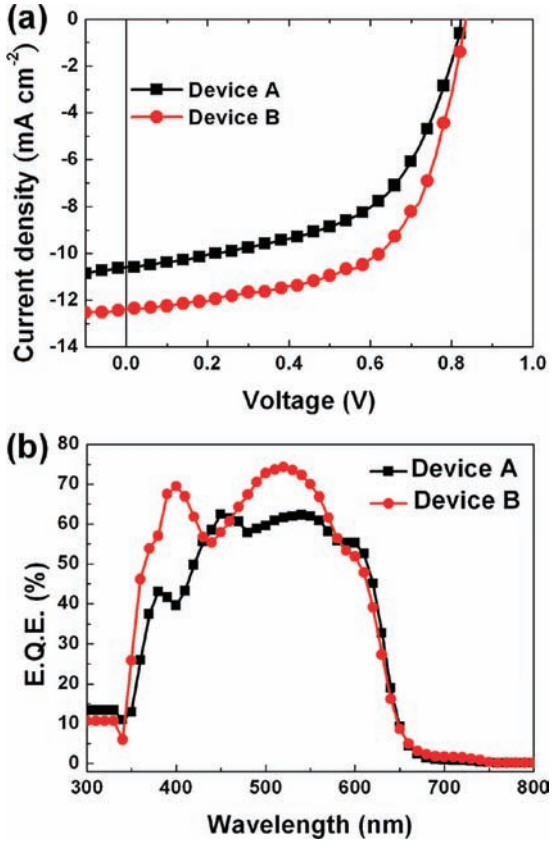

Figure 2. (a) Current density−voltage characteristics of device **A** (ITO/ZnO/ICBA:P3HT/PEDOT:PSS/Ag) and device **B** (ITO/ZnO/C-PCBSD/P3HT:ICBA/PEDOT:PSS/Ag) under illumination of AM 1.5G at 100 mW/cm^2. (b) External quantum efficiency of devices **A** and **B**.

We associate several factors with the observed improvements in device characteristics. Due to the lower surface energy of P3HT, as well as the excellent compatibility and the strong affinity between the fullerene analogues ICBA and C-PCBSD, the active layer deposited on C-PCBSD undergoes spontaneous vertical phase separation whereby the top surface becomes enriched with P3HT and the bottom contact becomes enriched with ICBA.[12] Such an inhomogeneous vertical gradient of the P3HT:ICBA blend benefits charge transport in the inverted configuration. Since ICBA is the major component in the active layer making contact with the bottom layer, the localized ICBA/C-PCBSD interface in device **B** plays a dominant role in determining the electron-extracting properties. Unlike the organic−inorganic ICBA/ZnO interface in device **A**, the fullerene-based organic−organic ICBA/C-PCBSD interface with intimate contact in device **B** enhances electrical coupling and lowers contact resistance. This facilitates electron transport and thereby reduces charge recombination losses at the interface. The higher LUMO energy level of ICBA is also beneficial in terms of energy alignment at the interface. The C-PCBSD LUMO energy level (−3.91 eV) is located between the LUMO of ICBA (−3.74 eV) and the conduction band of ZnO (−4.4 eV). Therefore, C-PCBSD functions as an intermediate in an energy gradient, so electrons in the ICBA domain can be efficiently extracted by C-PCBSD and transported to the ZnO through an energetically favorable pathway (Figure 1).[13]

To demonstrate the multifunctionality of the C-PCBSD interlayer in device **A**, a planar heterojunction device **C** (ITO/ZnO/ICBA/P3HT/PEDOT:PSS/Ag) and device **D** (ITO/ZnO/C-PCBSD/ICBA/P3HT/PEDOT:PSS/Ag) were each fabricated and investigated. Because such a simplified bilayer heterojunction completely excludes the influence of P3HT in the active layer, the macroscopic characteristics of devices **C** and **D** reflect the microscopic properties at the ICBA/ZnO interface in device **A** and the ICBA/C-PCBSD interface in device **B**, respectively. Figure 3 shows the $J-V$ characteristics of the planar heterojunction devices, both under AM 1.5G illumination and in the dark. Device **D** delivered $V_{oc} = 0.62$ V, $J_{sc} = 1.65$ mA/cm^2, FF = 51%, and a good PCE of 0.52%, greatly out-performing device **C**, producing $V_{oc} = 0.48$ V, $J_{sc} = 1.13$ mA/cm^2, FF = 41%, and 0.22% PCE.

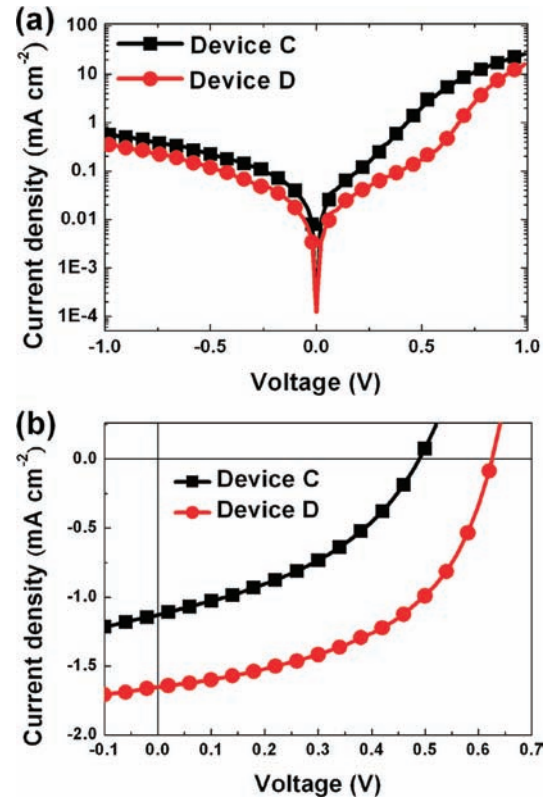

Figure 3. (a) Semilogarithmic plots of $J-V$ characteristics of heterojunction solar cell devices **C** and **D** in the dark and (b) linear plots under AM 1.5G illumination at 100 mW/cm^2.

Notably, the series resistance (R_s) of device **D** (60 Ω cm^2) is substantially decreased compared to that of device **C** (119 Ω cm^2),

confirming that the C-PCBSD interlayer is capable of reducing contact resistance to facilitate electron transport across the device. This is further demonstrated by the significant improvement in FF and J_{sc} values for device **C**. Furthermore, device **D**, with a C-PCBSD interlayer, showed a reduction in dark current under reverse bias (Figure 3a). This result suggests that the C-PCBSD interlayer in device **D** can also passivate the local shunts at the ZnO interface, thereby blocking the injection of holes in the leakage pathways of the ZnO.

Table 1. Characteristics of Devices **A**−**D**

device[a]	V_{oc} [V]	J_{sc} [mA/cm^2]	FF [%]	PCE [%]	R_s [Ω cm^2]
A	0.82	10.6	55	4.81	19.9
B	0.84	12.4	60	6.22	10.3
C	0.48	1.13	41	0.22	119
D	0.62	1.65	51	0.52	60

[a] Configurations: device **A**, ITO/ZnO/ICBA:P3HT/PEDOT:PSS/Ag; device **B**, ITO/ZnO/C-PCBSD/ICBA:P3HT/PEDOT:PSS/Ag; device **C**, ITO/ZnO/ICBA/P3HT/PEDOT:PSS/Ag; device **D**, ITO/ZnO/C-PCBSD/ICBA/P3HT/PEDOT:PSS/Ag.

The PCEs of the unencapsulated inverted solar cell device **B** were periodically measured for 21 days to monitor their long-term stability (Figure 4). Device **B** retains 87% of the magnitude of its original PCE value after being exposed to ambient conditions for 21 days. This explicitly demonstrates the superior air stability of inverted solar cells.

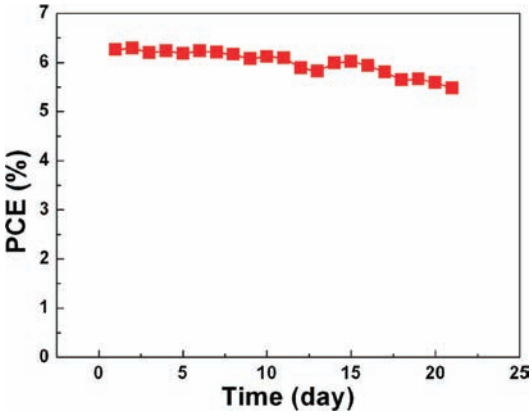

Figure 4. PCE values as a function of time for device **B** stored for 21 days under ambient conditions.

In conclusion, ICBA, possessing a high-lying LUMO energy level, has been utilized as the acceptor in a P3HT-based inverted PSC, exhibiting a high V_{oc} of 0.82 V that leads to a high PCE of 4.81%. Incorporation of an electron-extracting C-PCBSD interlayer into the ICBA:P3HT-based device further modulates the electronic and orbital interactions at the interface to improve the J_{sc} and FF, boosting the PCE to a record high 6.2%. To the best of our knowledge, this is the first example of an inverted PSC exceeding 5% PCE. This value is comparable to those reported for state-of-the-art conventional solar cells using novel low-band-gap conjugated polymers.[3] In view of the fact that the high-efficiency of P3HT-based PSCs is easily reproducible and insensitive to the thickness of the active layer, our development using the ICBA:P3HT system is very significant and shows potential for future commercialization. We also envisage that this promising strategy will provide an alternative route for developing high-performance tandem cells with inverted configurations.

Acknowledgment. This work was supported by the National Science Council and "ATP Plan" of the National Chiao Tung University and Ministry of Education, Taiwan. Y.H. and Y.L. thank the NSFC (Nos. 50633050 and 20821120293) for financial support.

Supporting Information Available: Details of device fabrication and characterization. This material is available free of charge via the Internet at http://pubs.acs.org.

References

(1) (a) Yu, G.; Gao, J.; Hummelen, J. C.; Wudl, F.; Heeger, A. J. *Science* **1995**, *270*, 1789. (b) Thompson, B. C.; Frechet, J. M. J. *Angew. Chem., Int. Ed.* **2008**, *47*, 58. (c) Günes, S.; Neugebauer, H.; Sariciftci, N. S. *Chem. Rev.* **2007**, *107*, 1324. (d) Cheng, Y.-J.; Yang, S.-H.; Hsu, C.-S. *Chem. Rev.* **2009**, *109*, 5868.

(2) (a) Woo, C. H.; Thompson, B. C.; Kim, B. J.; Toney, M. F.; Frechet, J. M. J. *J. Am. Chem. Soc.* **2008**, *130*, 16324. (b) Reyes-Reyes, M.; Kim, K.; Carroll, D. L. *Appl. Phys. Lett.* **2005**, *87*, 083506. (c) Li, G.; Shrotriya, V.; Huang, J.; Yao, Y.; Moriarty, T.; Emery, K.; Yang, Y. *Nat. Mater.* **2005**, *4*, 864. (d) Ma, W.; Yang, C.; Gong, X.; Lee, K.; Heeger, A. J. *Adv. Funct. Mater.* **2005**, *15*, 1617.

(3) (a) Huo, L.; Hou, J.; Zhang, S.; Chen, H.-Y.; Yang, Y. *Angew. Chem., Int. Ed.* **2010**, *49*, 1500. (b) Hou, J.; Chen, H.-Y.; Zhang, S.; Li, G.; Yang, Y. *J. Am. Chem. Soc.* **2008**, *130*, 16144. (c) Zou, Y.; Naiari, A.; Berrouard, P.; Beaupre, S.; Aich, B. R.; Tao, Y.; Leclerc, M. *J. Am. Chem. Soc.* **2010**, *132*, 5330. (d) Liang, Y.; Wu, Y.; Feng, D.; Tsai, S.-T.; Son, H.-J.; Li, G.; Yu, L. *J. Am. Chem. Soc.* **2009**, *131*, 56. (e) Qin, R.; Li, W.; Li, C.; Du, C.; Veit, C.; Schleiermacher, H.-F.; Adersson, M.; Bo, Z.; Liu, Z.; Inganas, O.; Wuerfel, U.; Zhang, F. *J. Am. Chem. Soc.* **2009**, *131*, 14612. (f) Chen, H.-Y.; Hou, J.; Zhang, S.; Liang, Y.; Yang, G.; Yang, Y.; Yu, L.; Wu, Y.; Li, G. *Nat. Photon.* **2009**, *3*, 649. (g) Hou, J.; Chen, H.-Y.; Zhang, S.; Chen, R. I.; Yang, Y.; Wu, Y.; Li, G. *J. Am. Chem. Soc.* **2009**, *131*, 15586. (h) Park, S. H.; Roy, A.; Beaupre, S.; Cho, S.; Coates, N.; Moon, J. S.; Moses, D.; Leclerc, M.; Lee, K.; Heeger, A. J. *Nat. Photon* **2009**, *3*, 297. (i) Liang, Y.; Xu, Z.; Xia, J.; Tsai, S.-T.; Wu, Y.; Li, G.; Ray, C.; Yu, L. *Adv. Mater.* **2010**, *22*, E135. (j) Huang, F.; Chen, K.-S.; Yip, H.-L.; Hau, S. K.; Acton, O.; Zhang, Y.; Luo, J.; Jen, A. K.-Y. *J. Am. Chem. Soc.* **2009**, *131*, 13886. (k) Wang, E.; Wang, L.; Lan, L.; Luo, C.; Zhuang, W.; Peng, J.; Cao, Y. *Appl. Phys. Lett.* **2008**, *92*, 033307.

(4) (a) Li, G.; Chu, C.-W.; Shrotriya, V.; Huang, J.; Yang, Y. *Appl. Phys. Lett.* **2006**, *88*, 253503. (b) Liao, H.-H.; Chen, L.-M.; Xu, Z.; Li, G.; Yang, Y. *Appl. Phys. Lett.* **2008**, *92*, 173303.

(5) (a) Mor, G. K.; Shankar, K.; Paulose, M.; Varghese, O. K.; Grimes, C. A. *Appl. Phys. Lett.* **2007**, *91*, 152111. (b) Waldauf, C.; Morana, M.; Denk, P.; Schilinsky, P.; Coakley, K.; Choulis, S. A.; Brabec, C. J. *Appl. Phys. Lett.* **2006**, *89*, 233517. (c) White, M. S.; Olson, D. C.; Shaheen, S. E.; Kopidakis, N.; Ginley, D. S. *Appl. Phys. Lett.* **2006**, *89*, 143517. (d) Steim, R.; Choulis, S. A.; Schilinsky, P.; Brabec, C. J. *Appl. Phys. Lett.* **2008**, *92*, 093303. (e) Wang, T.; Cai, W.; Qin, D.; Wang, E.; Lan, L.; Gong, X.; Peng, J.; Cao, Y. *J. Phys. Chem. C* **2010**, *114*, 6849.

(6) (a) Hau, S. K.; Yip, H.-L.; Baek, N. S.; Zou, J.; O'Malley, K.; Jen, A. K.-Y. *Appl. Phys. Lett.* **2008**, *92*, 253301. (b) Hau, S. K.; Yip, H.-L.; Acton, O.; Baek, N. S.; Ma, H.; Jen, A. K.-Y. *J. Mater. Chem.* **2008**, *18*, 5113. (c) Hau, S. K.; Yip, H.-L.; Ma, H.; Jen, A. K.-Y. *Appl. Phys. Lett.* **2008**, *93*, 233304.

(7) (a) Tao, C.; Ruan, S.; Zhang, X.; Xie, G.; Shen, L.; Kong, X.; Dong, W.; Liu, C.; Chen, W. *Appl. Phys. Lett.* **2008**, *93*, 193307. (b) Kyaw, A. K. K.; Sun, X. W.; Jiang, C. Y.; Lo, G. Q.; Zhao, D. W.; Kwong, D. L. *Appl. Phys. Lett.* **2008**, *93*, 221107.

(8) Chen, F.-C.; Wu, J.-L.; Hung, Y. *Appl. Phys. Lett.* **2010**, *96*, 193304.

(9) Kim, B. J.; Miyamoto, Y.; Ma, M.; Frechet, J. M. J. *Adv. Funct. Mater.* **2009**, *19*, 1173.

(10) Hsieh, C.-H.; Cheng, Y.-J.; Li, P.-J.; Chen, C.-H.; Dubosc, M.; Liang, R.-M.; Hsu, C.-S. *J. Am. Chem. Soc.* **2010**, *132*, 4887.

(11) (a) He, Y.; Chen, H.-Y.; Hou, J.; Li, Y. *J. Am. Chem. Soc.* **2010**, *132*, 1377. (b) Zhao, G.; He, Y.; Li, Y. *Adv. Mater.* **2010**, *22*, 4355.

(12) (a) Campoy-Quiles, M.; Ferenczi, T.; Agostinelli, T.; Etchegoin, P. G.; Kim, Y.; Anthopoulos, T. D.; Stavrinou, P. N.; Bradley, D. D. C. *Nat. Mater.* **2008**, *7*, 158. (b) Xu, Z.; Chen, L.-M.; Yang, G.; Huang, C.-H.; Hou, J.; Wu, Y.; Li, G.; Hsu, C.-S.; Yang, Y. *Adv. Funct. Mater.* **2009**, *19*, 1227.

(13) Niu, Y.-H.; Liu, M. S.; Ka, J. W.; Jen, A. K.-Y. *Appl. Phys. Lett.* **2006**, *88*, 093505.

JA108259N